AIMS Energy, 11(5): 896–917.
DOI: 10.3934/energy.2023043
Received: 01 August 2023
Revised: 11 September 2023
Accepted: 14 September 2023
Published: 22 September 2023

http://www.aimspress.com/journal/energy

Research article

Remaining useful life indirect prediction of lithium-ion batteries using CNN-BiGRU fusion model and TPE optimization

Xiaoyu Zheng[1,2], Dewang Chen[1,2,3]*, Yusheng Wang[3] and Liping Zhuang[4]

[1] School of Transportation, Fujian University of Technology, 69-1 Xuefu South Road, Fuzhou, 350118, China
[2] Intelligent Transportation System Research Center, Fujian University of Technology, 69-1 Xuefu South Road, Fuzhou 350118, China
[3] College of Mathematics and Computer Science, Fuzhou University, 2 Xueyuan Road, Fuzhou, 350108, China
[4] School of Electronics, Electrical Engineering and Physics, Fujian University of Technology, 69 Xuefu South Road, Fuzhou, 350118, China

* **Correspondence:** Email: dwchen@fjut.edu.cn.

Abstract: The performance of lithium-ion batteries declines rapidly over time, inducing anxiety in their usage. Ascertaining the capacity of these batteries is difficult to measure directly during online remaining useful life (RUL) prediction, and a single deep learning model falls short of accuracy and applicability in RUL predictive analysis. Hence, this study proposes a lithium-ion battery RUL indirect prediction model, fusing convolutional neural networks and bidirectional gated recurrent units (CNN-BiGRU). The analysis of characteristic parameters of battery life status reveals the selection of pressure discharge time, average discharge voltage and average temperature as health factors of lithium-ion batteries. Following this, a CNN-BiGRU model for lithium-ion battery RUL indirect prediction is established, and the Tree-structured Parzen Estimator (TPE) adaptive hyperparameter optimization method is used for CNN-BiGRU model hyperparameter optimization. Overall, comparison experiments on single-model and other fusion models demonstrate our proposed model's superiority in the prediction of RUL in terms of stability and accuracy.

Keywords: lithium-ion battery; RUL; CNN-BiGRU; indirect prediction; deep learning

1. Introduction

Due to the emerging energy crisis, there is a growing imperative for societies to explore and develop new energy sources. Lithium-ion batteries have gained momentum in the new energy market owing

to their high energy density, high output voltage, long cycle life, and wide operating temperature range [1–3]. Nonetheless, the internal resistance of lithium-ion batteries rises with repeated cycles of charging and discharging, which results in serious heating that undermines the performance and normal functioning of the battery pack [4, 5]. The remaining useful life (RUL) of a lithium-ion battery defines the number of charging and discharging cycles remaining between its beginning of measurement and the end-of-life (EOL) [6]. A regular RUL prediction of lithium-ion batteries can reveal the number of remaining useful cycles, approximate the proximity of a battery to EOL and prevent potential risks associated with its usage [7–11]. Consequently, the accuracy of the RUL evaluation method for lithium-ion batteries has a direct bearing on the overall performance of the battery management system, which is of immense practical significance in the field of energy battery applications.

The traditional life prediction model is a demanding and stringent process owing to the intricate physical and chemical attributes of lithium-ion batteries. Fortunately, the RUL model of lithium-ion batteries built on data-driven technology is a potent and efficacious approach facilitated by the progress of Artificial Intelligence. This method treats a battery as a black box, bypasses the intricate internal changes it undergoes and identifies the statistical pattern through the historical measurement dataset, which enables the prediction of RUL in lithium-ion batteries. Recent years have witnessed an increasing number of scholars focusing on power batteries research. There exist two principal categories for developing battery life prediction models: model-based and data-driven approaches [12–14].

The model-based method is often utilized to establish a mathematical model of a battery, as it involves analyzing the battery's physical structure and electrochemical reaction and estimating the changing process of battery parameters. For example, Khare et al. [15] used a statistical modeling method to map the internal resistance of a battery to its health state, while Mevawalla et al. [16] developed an equivalent circuit model incorporating physio-chemical theory and a nonlinear equation for the internal resistance to simulate the internal resistance and surface temperature of lithium-ion batteries using measurable parameters. Wang et al. [17] proposed a resistance-based thermal model of batteries, while Xie et al. [18] suggested a distributed spatial-temporal online correction algorithm for state of charge three-dimensional state of temperature (SOT) co-estimation of a battery. Xing et al. [19] used a fusion prediction method based on the physics of failure (PoF) and data-driven technology to analyze the failure mechanism caused by changes in the battery's physical and chemical characteristics. Wang et al. [20] introduced a spherical particle filter to predict the RUL of lithium-ion batteries by solving the state space model and evaluating the capacity degradation. Similarly, Tran et al. [21] investigated and compared the performance of three different equivalent circuit models for four lithium-ion battery chemistries under dynamic and non-dynamic current profiles. However, while the model-based method has proven effective, it is susceptible to bad external conditions and may not establish an accurate mechanism model. Additionally, the diverse physical and chemical properties of various batteries weaken the model's applicability, necessitating modifications to suit different batteries, which is a difficult task.

The data-driven method involves utilizing techniques such as machine learning to extract battery ageing characteristics from battery data collected during operation, revealing the relationship between the input data and the degradation process and predicting the remaining battery life [22–24]. For example, Kim et al. [25] proposed strategically switched metaheuristics to fully exploit the shape of an objective function around sample points. Cai et al. [26] proposed an optimization process based

on a nondominated sorting genetic algorithm (NSGA II), short-term characteristics of support vector regression (SVR), and current pulse test for prediction. Qin et al. [27] established an improved particle swarm optimization-support vector regression (PSO-SVR) model for estimating RUL under different fault thresholds. Similarly, Cai et al. [28] proposed a hybrid data-driven algorithm to reconstruct the phase space, predict RUL by combining discrete gray model (DGM), relevance vector machine (RVM), and artificial fish swarm algorithm (AFSA). Various studies have applied deep learning to improve prediction accuracy. For instance, Fei et al. [29] proposed a novel deep learning-based framework, a bilateral branched Visual Transformer with Dilated Self-Attention, for online state of health (SOH) estimation. Ma et al. [30] and Zhang et al. [31] used long short-term memory (LSTM) to predict RUL, while Yalçın et al. [32] proposed convolutional neural network (CNN) artificial bee colony (ABC) to estimate heat generation rate (HGR) and voltage. Wang et al. [33] proposed a transferable lithium-ion battery RUL prediction method, while Chen et al. [34] presented a fusion model based on CNN and LSTM, and Xia et al. [35] proposed a hybrid prediction model based on LSTM and fully connected layer to capture the correlation in earlier data. However, these data-driven methods have complex structure, entail extensive calculations and prolonged training times, which remain a challenge.

It is not possible to predict the RUL of lithium-ion batteries accurately after measuring all the properties owing to the fact that the battery cycle enters the next stage after manual measurement, which alters the RUL and makes the predicted value insignificant. In order to achieve online RUL prediction, it is necessary to find surrogate properties that are easily measurable to establish indirect health factors, as well as predict the feature variables used for the prediction alongside the RUL. Therefore, it is important to design a real-time prediction model architecture to achieve online RUL prediction in the true sense. In this study, we combine CNN and bidirectional gated recurrent units (BiGRU) models to predict the RUL of lithium-ion batteries. The main contributions of this paper are as follows.

1.In practical applications, it is difficult to obtain direct health factors of lithium batteries in real time, such as capacity [36]. Therefore, in this study, we extracted indirect health factors of lithium batteries, including isothermal discharge time, average voltage, and average temperature and analyzed the effectiveness of health factor selection through Pearson correlation coefficient.

2.To improve the limited prediction accuracy of a single recurrent neural network, we proposed a CNN-BiGRU model for indirectly predicting the RUL of lithium batteries. We used a convolutional neural network to extract the latent features of battery health factors, and fitted these features using bidirectional gated recurrent units to enhance the RUL prediction accuracy of lithium batteries.

3.We introduced the Tree-structured Parzen Estimator (TPE) hyperparameter optimization method to optimize the hyperparameters of the proposed model. Compared to the CNN, GRU, and BiGRU models, the CNN-BiGRU model with TPE hyperparameter optimization does not require manual parameter tuning and achieves higher RUL prediction accuracy for lithium-ion batteries.

The rest of this paper is organized as follows. Section two describes the RUL prediction problem of lithium-ion batteries and the data structure. Then, in section three, the details of the proposed approach are introduced. And section four, the proposed model is compared with the GRU model, BiGRU model, CNN-GRU model, and the all-around performance of each model in the RUL prediction experiment are analyzed. Finally, the conclusion is presented in section five.

2. Problem statement of RUL prediction of lithium-ion batteries

2.1. The problem of RUL prediction of lithium-ion batteries

The RUL of a lithium-ion battery is the number of charge/discharge cycles remaining between the start of the measurement and the threshold of failure, and its calculation formula is obtained by Eq (1).

$$RUL = Cycle - Cycle_{EOL} \tag{1}$$

Where, $Cycle$ is the charge/discharge cycles of the lithium-ion battery at the measurement moment, and $Cycle_{EOL}$ is the charge/discharge cycles of the lithium-ion battery at the failure threshold. The lithium-ion battery degradation to a certain level will affect normal use, and 70% of the standard capacity of lithium-ion batteries is usually used as the failure threshold in research [37].

2.2. Data set

This paper uses the lithium-ion battery data set from the NASA Ames Prognostics Center of Excellence [38]. The LiCoO2 is used as the positive material, soft and hard carbon as the negative material and lithium salt as the electrolyte material for the 18,650 lithium-ion cobalt acid battery. The battery has a rated capacity of 2 Ah and a rated voltage of 4.2 V. Lithium-ion batteries are charged (C-rate = 0.75 C), discharged (C-rate = 1 C) and tested for impedance at different temperatures until the end of the battery life and recorded for collected data, such as voltage, current, temperature and impedance. Table 1 shows the details of the NASA battery pack. We took the first group of lithium-ion batteries as an example to introduce the process of the NASA battery pack ageing life test. The charging process consists of charging with a constant current (CC) mode of 1.5 A until the voltage reaches 4.2 V, then the charging continues with a constant voltage (CV) mode until the charging current drops to 20 mA. The discharge process starts with a discharge with a CC of 2 A until the voltage of the battery reaches a different set value. For impedance measurements, the battery is scanned by electrochemical impedance spectroscopy (EIS) from 0.1 Hz to 5 kHz. The condition for the battery's EOL is that after recharging and discharging the lithium-ion battery repeatedly, the battery is considered invalid when its rated capacity decreases from 100% to 70% (from 2 Ah to 1.4 Ah). The EOL of lithium-ion batteries can be defined as the number of cycles when the capacity of the lithium-ion batteries drops to the failure threshold during the initial experiment.

Table 1. NASA battery pack details.

Group	Battery	Temperature(°C)	CC(A)	V_{cutoff}(V)	Cycle	Capacity (Ah)
Group 1	B0005	24	2	2.7	168	1.8565
	B0006			2.5	168	2.0353
	B0007			2.2	168	1.8911
	B0018			2.5	132	1.8550
Group 2	B0025	24	0/4	2.0	28	1.8470
	B0026			2.2	28	1.8133
	B0027			2.5	28	1.8233
	B0028			2.7	28	1.8047
Group 3	B0038	24,44	1	2.2	47	0.8981
	B0039		2	2.5	47	0.1190
	B0040		3	2.7	47	0.6735

3. Indirect RUL prediction model for lithium-ion batteries based on CNN-BiGRU

3.1. Extraction of health factors for lithium-ion batteries

Health factors can be used to characterize the health status and RUL of lithium-ion batteries [39]. Battery data contains information related to battery aging, and these aging-related features are referred to as health factors. Battery capacity and resistance can directly indicate battery aging and are known as direct health factors, while collected battery data such as current, voltage and temperature cannot directly indicate battery aging and are known as indirect health factors.

In practical measurements, battery capacity, which is a direct health factor, is typically estimated using the ampere-hour integration method and cannot be measured directly, while battery data such as current, voltage and temperature, which are indirect health factors, can be easily collected. Studies [40] have used the time of discharge with the same voltage drop in lithium-ion batteries as an indirect factor to predict their RUL, which has shown promising results. This paper builds upon this approach by adding two more indirect health factors, average temperature and average discharge voltage, and uses three indirect factors, average temperature, average discharge voltage and discharge time with the same voltage drop to predict the remaining discharge capacity of the battery and the remaining life of the lithium-ion battery indirectly. The formula for calculating the discharge time with the same voltage drop is given below:

$$\Delta t_{i(HI)} = t_{V_{\text{high}}} - t_{V_{\text{low}}}, i = 1, 2, 3, \ldots, k \tag{2}$$

Here, $t_{i(HI)}$ refers to the discharge time with the same voltage drop for the i-th cycle period, while $t_{V_{\text{high}}}$ represents the discharge time from the start of discharge to the high voltage V_{high} and $t_{V_{\text{low}}}$ represents the discharge time from the start of discharge to the low voltage V_{low}. For the NASA lithium-ion battery dataset, V_{high} of 3.7 V and V_{low} of 3.5 V were chosen for extracting the discharge time with the same voltage drop. Taking Battery B0005 as an example, the capacity versus cycle and discharge time with the same voltage drop versus cycle are shown in Figure 1.

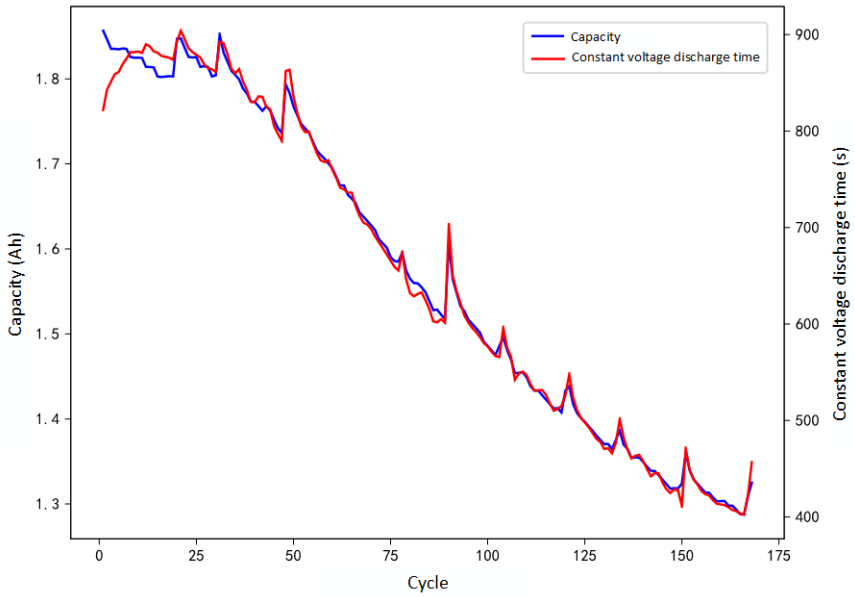

Figure 1. Capacity and constant voltage discharge time relationship diagram for battery B0005.

According to Figure 1, both the decay trends and the curves of capacity-cycles and isobaric discharge time-cycles are almost identical and overlapping. This study uses the mean discharge voltage, mean temperature and isobaric discharge time as the health factors. Pearson's correlation coefficient is used to measure the correlation between the selected health factors and capacity, proving the effectiveness of the selected health factors. The calculation formula of Pearson's correlation coefficient is shown in Eq (3).

$$\rho = \frac{\sum_{i=1}^{n}\left(X_i - \bar{X}\right)\left(Y_i - \bar{Y}\right)}{\sqrt{\sum_{i=1}^{n}\left(X_i - \bar{X}\right)^2}\sqrt{\sum_{i=1}^{n}\left(Y_i - \bar{Y}\right)^2}} \tag{3}$$

Table 2 presents the Pearson coefficients between the average discharge voltage, average temperature, constant voltage discharge time, and capacity for batteries B0005, B0006, and B0007. Table 3 provides an explanation of the battery health factors. Heat maps of the Pearson coefficients for the three batteries are shown in Figures 2(a) to 2(c). The Pearson coefficient values between the constant voltage discharge time and capacity for these three batteries, as depicted in Table 2, were found to be above 0.990, indicating a strong positive correlation. Moreover, the Pearson coefficient values between the average discharge voltage and capacity were also above 0.961, demonstrating a positive correlation between the two. The Pearson coefficient value between the average temperature and capacity was found to be above -0.588, signifying a relatively strong negative correlation.

In summary, it has been demonstrated that the extracted average discharge voltage, average temperature and constant voltage discharge time can effectively characterize the discharge capacity of lithium-ion batteries. This, in turn, lays the groundwork for the indirect prediction of the RUL of these batteries.

Table 2. The correlation coefficient table between battery health factors and capacity.

	B0005				B0006				B0007			
Variables	x1	x2	x3	x4	x1	x2	x3	x4	x1	x2	x3	x4
x1	1	0.982	–0.810	0.998	1	0.965	–0.823	0.990	1	0.961	–0.588	0.997
x2	0.982	1	–0.824	0.989	0.965	1	–0.843	0.989	0.961	1	–0.632	0.975
x3	–0.810	-0.824	1	–0.804	–0.823	–0.843	1	–0.831	–0.588	–0.632	1	–0.602
x4	0.998	0.989	–0.804	1	0.990	0.989	–0.831	1	0.997	0.975	–0.602	1

Table 3. Explanation of the meaning of battery health factors and capacity.

Variable	Explanation
x1	Battery capacity
x2	battery mean discharge voltage
x3	battery mean discharge temperature
x4	time taken for battery voltage to drop from 3.7V to 3.5V during discharge

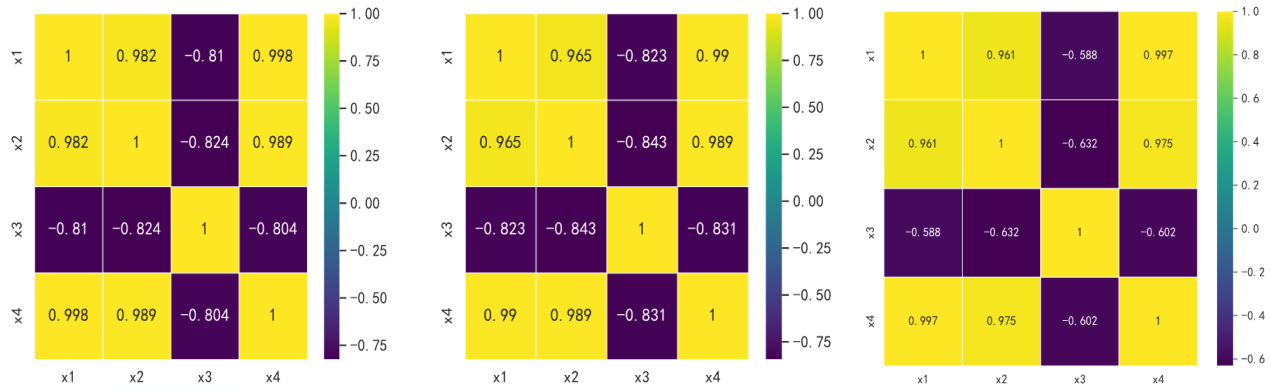

(a) B0005 (b) B0006 (c) B0007

Figure 2. Thermographic map of the correlation between battery health factors and capacity.

3.2. The fusion model of CNN-BiGRU

The prediction of time series problems concerning lithium-ion batteries using LSTM and GRU recurrent neural networks only considers the effects of past battery data on present battery data, and neglects the relationship between battery data and its propagation through the recurrent neural network. Integrating both the forward and backward propagations of relevant information, a BiGRU offers each data point access to historical and future information to improve prediction accuracy. This paper proposes a CNN-BiGRU fusion model that leverages a CNN as a feature extraction layer for battery data and a BiGRU as a prediction module, amalgamating the advantages of both models to increase prediction accuracy. The CNN-BiGRU fusion model follows the structure shown in Figure 3, composed of an input layer, a convolutional layer, a pooling layer, a BiGRU layer, a dropout layer and

a fully connected layer.

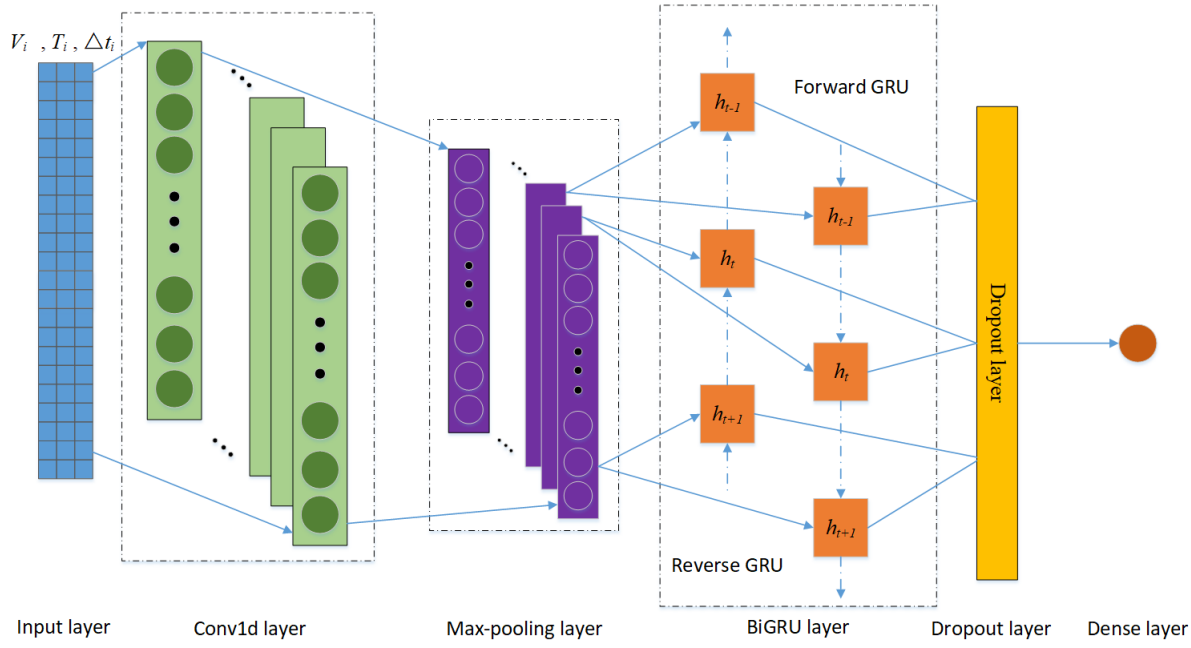

Figure 3. The architecture diagram of the CNN-BiGRU model.

The CNN-BiGRU model aims to predict the capacity of a lithium-ion battery based on health factors. The input layer of the model takes mean voltage, mean temperature and isothermal discharge time as input data. The health factors undergo one-dimensional convolution to identify potential information among them, followed by pooling to enhance the model features and reduce parameters. The output of the pooling layer goes through the BiGRU network that updates the state of the GRU and conducts battery capacity prediction using forward and backward propagation. To prevent overfitting, the output of the BiGRU layer is fed into a dropout layer that randomly disconnects neurons. The fully connected layer generates the final capacity prediction result. The model uses the ReLu activation function to avoid overfitting and provides nonlinear advantages. Figure 4 presents the algorithm flow chart of the CNN-BiGRU fusion model.

The detailed algorithm steps are described below. First, extract the raw lithium-ion battery data from the NASA Prognostics Center of Excellence open battery dataset. The data includes the cycle number N_i, discharge voltage V_i, discharge temperature T_i, battery capacity C_i, and the invalid data is filtered out. Second, calculate the average discharge voltage $\bar{V}_i$, average discharge temperature $\bar{T}_i$ and capacity C_i for each cycle based on the cycle number. Third, extract the discharge voltage data for each cycle and calculate the isothermal discharge time $\Delta t_{i(HI)}$ based on the preset V_{high} of 3.7 V and V_{high} of 3.5 V. Next, perform min-max normalization on the health factors, including the average discharge voltage $\bar{V}_i$, average discharge temperature $\bar{T}_i$, isothermal discharge time $\Delta t_{i(HI)}$ and capacity. Based on the principle of CNN multivariate single-step prediction, construct a three-dimensional array for data input in the format of [sample, stride, feature], and then split it into training and testing sets. Set up the hyperparameter configuration space for the CNN-BiGRU model and initialize the hyperparameters, including the number of convolutional filters, stride, kernel size, pooling size, number of GRU in the bidirectional layer, dropout rate, and learning rate. Optimize the hyperparameters using TPE, calculate

the suitable hyperparameter point and add it to the initial set of TPE collections. Repeat the above step until the maximum epoch times (set to 50 times) is reached or there is a depletion of resources. Lastly, input the testing set into the optimized CNN-BiGRU model for capacity prediction, and calculate the battery remaining life based on the predicted capacity and the battery failure threshold. Output the predicted remaining life of the battery.

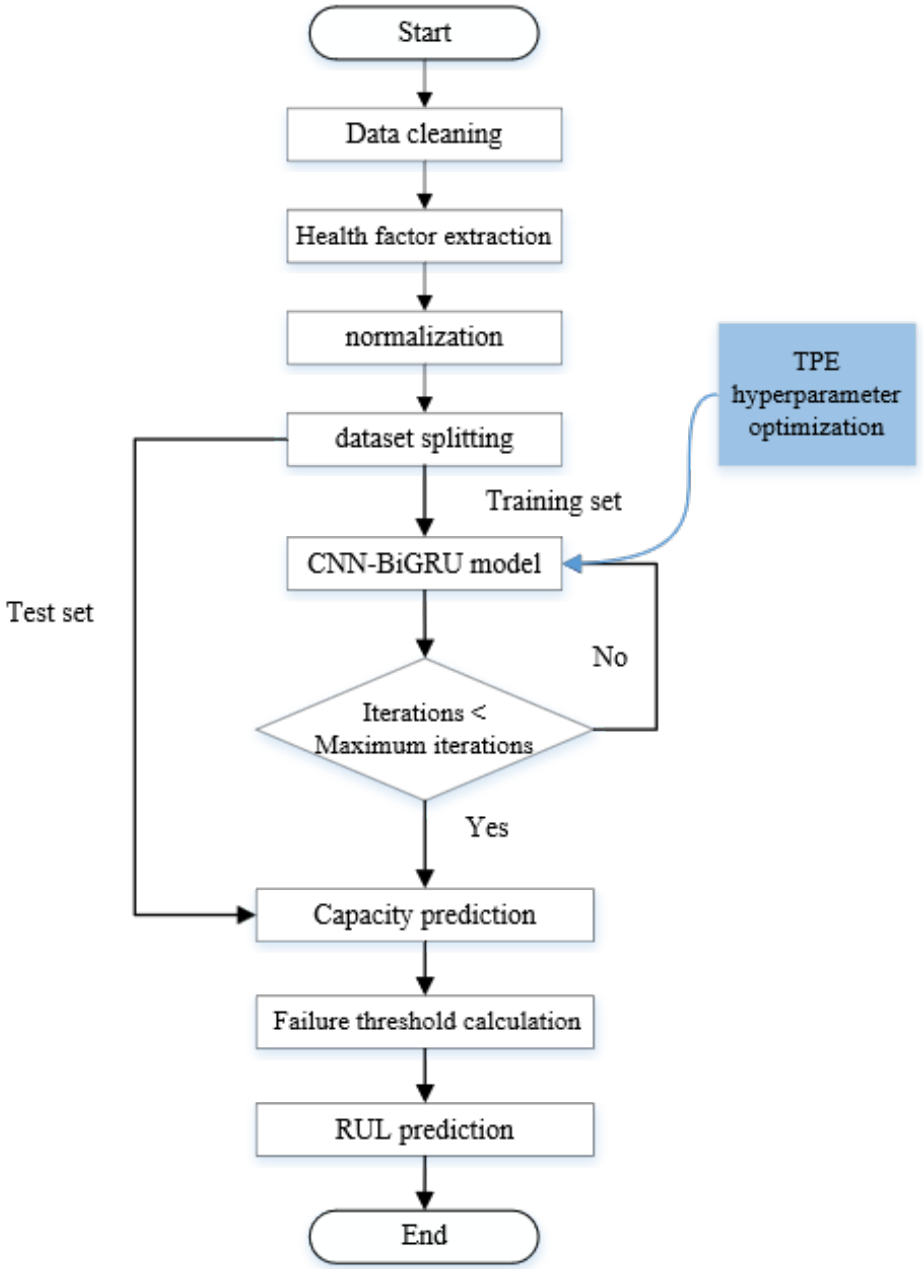

Figure 4. The flowchart of the CNN-BiGRU model.

4. Experiment

4.1. Model evaluation metrics

To evaluate the model's performance for predicting the RUL of a lithium-ion battery, the following evaluation metrics are used: mean absolute percentage error (MAPE), mean absolute error (MAE), mean squared error (MSE), root mean squared error (RMSE), absolute error (AE) and relative error (RE).

$$MAPE = \frac{1}{N}\sum_{i=1}^{N}\left|\frac{C_{\text{pred}}(i) - C_{\text{tue}}(i)}{C_{\text{true}}(i)}\right| \times 100\% \tag{4}$$

$$RMSE = \left(\frac{1}{N}\sum_{i=1}^{N}\left(C_{\text{pred}}(i) - C_{\text{true}}(i)\right)^2\right)^{1/2} \tag{5}$$

$$MAE = \frac{1}{N}\sum_{i=1}^{N}\left|\frac{C_{\text{pred}}(i) - C_{\text{true}}(i)}{C_{\text{true}}(i)}\right| \tag{6}$$

$$MSE = \frac{1}{N}\sum_{i=1}^{N}\left(C_{\text{pred}}(i) - C_{\text{true}}(i)\right)^2 \tag{7}$$

$$AE = |RUL_{\text{pred}} - RUL_{\text{true}}| \tag{8}$$

$$RE = |RUL_{\text{pred}} - RUL_{\text{true}}|/RUL_{\text{true}} \tag{9}$$

Where $C_{\text{pred}}(i)$ for predicted capacity value, $C_{\text{true}}(i)$ for true capacity value, N for cycle number, RUL_{pred} for predicted remaining life value and RUL_{true} for true remaining life value. MAPE and RMSE are the accuracy metrics for capacity prediction and the lower the value, the more accurate the capacity prediction. AE and RE reflect the performance metrics of the model for RUL prediction and the closer to zero the values, the more accurate the RUL prediction.

4.2. TPE hyperparameter optimization algorithm

Hyperparameters have a significant impact on the accuracy of predictive models [41,42]. When the model is relatively simple, the hyperparameter search space, and the dataset are both small, optimizing the objective function that can be used as a key way to search and adjust hyperparameters. However, as the model used in this paper is a deep learning model, although the objective function of deep learning models can be easily obtained, the training process is time-consuming. If the objective function is chosen as the optimization method for hyperparameter search, it will result in longer computation time and lower efficiency.

The Bayesian optimization algorithm for hyperparameters is a method that uses a surrogate function instead of the objective function to indirectly provide the optimal combination of hyperparameters for the objective function by calculating the performance of hyperparameters on the surrogate function. The TPE algorithm is a Bayesian optimization algorithm, as well as a model-based sequential global optimization algorithm. The core of this algorithm is to (1) determine

the search space of hyperparameters (2) determine the objective function to be optimized (3) determine the surrogate function of the objective function (4) use a suitable acquisition function as the position of the next prediction point, and (5) update the surrogate function and store the previous calculation process.

The TPE algorithm constructs a graph search space consisting of hyperparameters, such as the number of convolutional filters, stride, kernel size, number of GRU in the bidirectional layer, dropout rate, and learning rate. The hyperparameter combination space is usually composed of Gaussian distribution N, uniform distribution U, log-uniform distribution $logU$ or categorical variables. Table 4 shows the prior distribution of hyperparameters used in this paper. Let x represent the set of hyperparameters, y is the evaluation value under x and TPE models likelihood probability $p(x \mid y)$ and a priori probability $p(y)$.

Table 4. The prior distribution of hyperparameter.

Hyperparameter type	Symbol	Prior distribution
Number of convolution kernels	k	$LogU(70, 1.25)$
Stride	s	$LogU(3.6, 1.2)$
Convolution kernel size	f	$LogU(4.5, 1.3)$
Number of bidirectional gated recurrent units	h	$LogU(100, 1.33)$
Dropout rate	p	$LogU(0.05, 0.5)$
Batch size	b	$LogU(22, 1.3)$
Learning rate	a	$LogU(0.0007, 1.3)$

TPE converts prior probability distributions to generate a series of hyperparameter combination spaces under which different density distributions are produced. When the prior distribution is a logarithmic uniform distribution, TPE will convert it into an exponentially truncated Gaussian distribution; when the prior distribution is uniform, TPE will convert it into a truncated Gaussian distribution; and when the prior distribution is categorical, TPE will transform it into a reweighted categorical distribution. This process generates a range of hyperparameter spaces and a series of density distributions.

To demonstrate the effectiveness of TPE hyperparameter optimization, we used the CNN-BiGRU model with battery B0005 as an example. We specified the range of hyperparameters to be searched using the TPE optimization algorithm to find the optimal combination. Table 5 shows the experimental results of the TPE optimization algorithm applied to battery B0005.

As illustrated in Table 5, the TPE algorithm achieved a minimum error of 0.69% after 25 epochs, with a final accuracy of 99.31%. This error percentage was within 0.7%, indicating the effectiveness of the TPE hyperparameter search. Table 6 provides detailed hyperparameters and corresponding accuracies for each epoch of the TPE algorithm, and readers are referred to Table 4 for symbol explanations.

Table 6 shows that the optimal hyperparameter combination was achieved after 25 epochs, with the following values: 51 convolutional kernels k, stride s of two, kernel size f of two, 342 BiGRU neurons h, 0.0982 dropout rate p, batch size b of 43 and learning rate a of 0.0005.

Table 5. Experimental results of TPE on battery B0005.

Epochs	Error	Epochs	Error	Epochs	Error	Epochs	Error	Epochs	Error
1	4.05	11	2.61	21	1.26	31	2.18	41	5.66
2	3.50	12	7.24	22	6.40	32	2.30	42	3.75
3	2.34	13	4.35	23	1.25	33	4.40	43	4.41
4	8.51	14	2.18	24	2.77	34	4.84	44	7.79
5	2.28	15	2.56	25	0.69	35	3.13	45	1.32
6	1.84	16	4.67	26	1.55	36	2.81	46	2.91
7	5.41	17	6.17	27	3.63	37	5.21	47	1.92
8	3.54	18	3.99	28	2.59	38	2.61	48	3.75
9	3.37	19	2.07	29	4.21	39	1.15	49	3.89
10	1.12	20	1.88	30	2.18	40	4.22	50	2.02

Table 6. Hyperparameter combinations of TPE on battery B0005.

Epochs	k	s	f	h	p	b	a	Error
1	66	3	4	101	0.1305	20	0.0008	4.05%
2	45	5	4	121	0.0736	24	0.0008	3.50%
3	43	4	4	197	0.0751	29	0.0007	2.34%
4	71	4	5	108	0.0273	24	0.0010	8.51%
5	102	4	4	117	0.0589	20	0.0005	2.28%
...	...	...	...	...	...	...	...	...
25	51	2	2	342	0.0982	43	0.0005	0.69%
...	...	...	...	...	...	...	...	...
50	66	6	3	97	0.0280	23	0.0007	2.02%

The model was then tested using both the default hyperparameters and the TPE-optimized hyperparameters. Table 7 shows the experimental results.

Table 7 shows that using TPE to optimize the hyperparameters reduced the error of the CNN-BiGRU model to 0.69%, while using the default hyperparameters resulted in an error of 1.10%. These results demonstrate that TPE hyperparameter optimization is effective in controlling the error of the CNN-BiGRU model within 0.7% and can improve performance by 59.4%.

Table 7. The comparison between TPE-optimized hyperparameter combination and default hyperparameter combination.

Type	k	s	f	h	p	b	a	Error
TPE optimization	51	2	2	342	0.0982	43	0.0005	0.69%
default	128	1	1	256	0.3	10	0.0010	1.10%

4.3. Result and analysis

We conducted RUL prediction experiments on three batteries, B0005, B0006, and B0007, using their average discharge voltage $\bar{V}_i$, average discharge temperature $\bar{T}_i$ and isothermal discharge time as features to establish the relationship between the features and their capacity. The hyperparameters of the CNN-BiGRU model established using TPE hyperparameter search are shown in Table 8.

Table 8 shows the parameters of the CNN-BiGRU model established using TPE hyperparameter optimization for battery B0005 as an example. The same parameters were used for the other two batteries. The prediction starting point for battery B0005 was 60, and the model parameters after TPE hyperparameter optimization were as follows: 51 convolutional kernels k, stride s of two, kernel size f of two, 342 BiGRU neurons h, 0.0982 dropout rate p, batch size b of 43 and learning rate a of 0.0005.

Table 8. The comparison between TPE-optimized hyperparameter combination and default hyperparameter combination.

Battery	Starting point	k	s	f	h	p	b	a
B0005	60	51	2	2	342	0.0982	43	0.0005
B0005	84	126	3	1	934	0.1028	20	0.0010
B0005	100	28	4	9	236	0.2726	24	0.0010
B0006	60	53	2	6	581	0.0459	19	0.0010
B0006	84	58	3	4	419	0.0459	21	0.0006
B0006	100	66	3	2	78	0.0420	21	0.0010
B0007	60	60	4	5	78	0.0320	18	0.0010
B0007	84	64	3	4	101	0.0801	33	0.0010
B0007	100	79	3	3	112	0.0825	25	0.0010

The model parameter settings for the other compared algorithms are listed below. The models compared in this study are CNN-GRU, CNN-BiGRU, GRU, and BiGRU. The CNN-GRU model is similar to the CNN-BiGRU structure shown in Figure 3, but it replaces the BiGRU layer with a GRU layer. In the case of batteries B0005 and B0006, the CNN-GRU model has 128 convolutional kernels with a size of one and a pooling layer with a size of two, and 120 GRU cells. In contrast, for battery B0007, the CNN-GRU model predicts 60 different times, and each prediction uses a different set of hyperparameters. The number of convolutional kernels varies from 32 to 64, while the number of GRU cells remains constant at 128.

The structure of the GRU model comprises a GRU layer, a dropout layer and a fully connected layer. The dropout rate for each battery is set to 0.3, and the number of GRU cells varies. For batteries B0005 and B0006, the GRU model has 150 cells, whereas for battery B0007, it has 200 cells. The BiGRU model's structure is similar to that of the GRU model, but with a BiGRU layer instead of the GRU layer. The number of BiGRU cells varies across batteries: 100 cells for batteries B0005 and B0006 and 200 cells for battery B0007. In Figures 5 (a) to (i), the capacity prediction results of the CNN-BiGRU model, along with those of the CNN-GRU, GRU and BiGRU models, are shown for three batteries. The figures compare the different models' performance in predicting battery capacity, which is an essential aspect of battery health management.

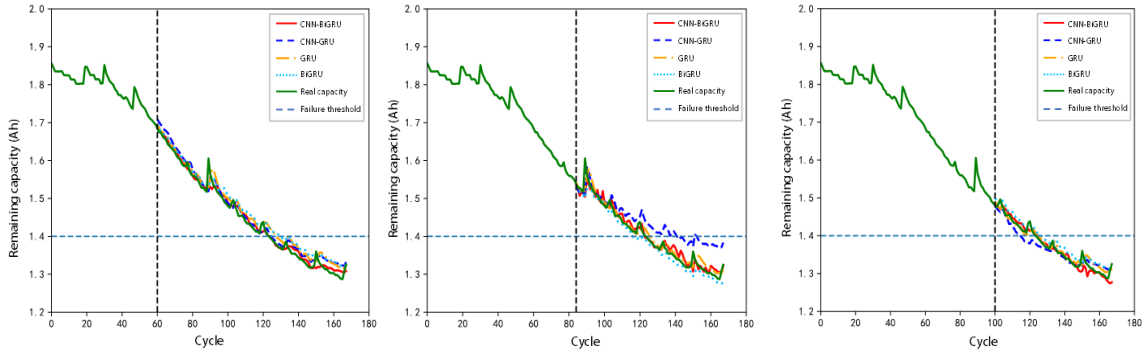

(a) B0005 with prediction starting point of 60 (b) B0005 with prediction starting point of 84 (c) B0005 with prediction starting point of 100

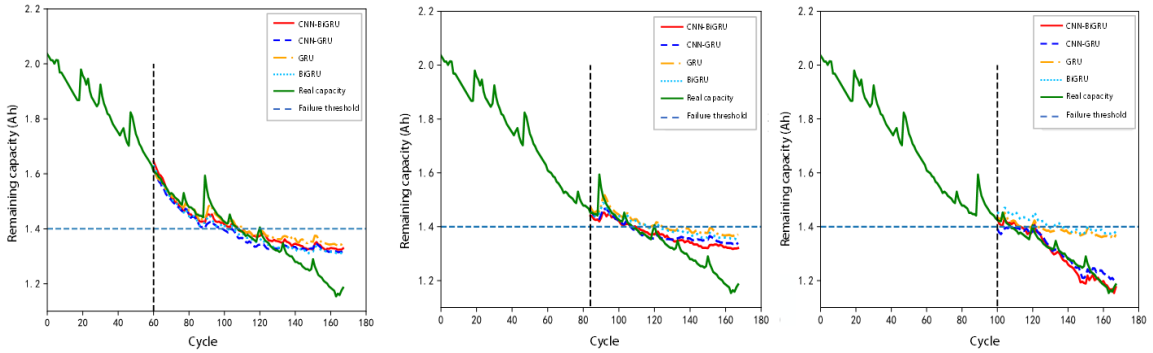

(d) B0006 with prediction starting point of 60 (e) B0006 with prediction starting point of 84 (f) B0006 with prediction starting point of 100

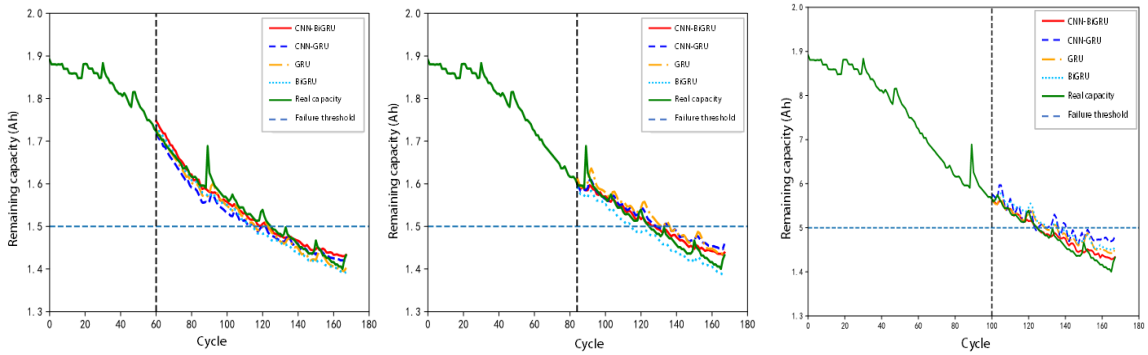

(g) B0007 with prediction starting point of 60 (h) B0007 with prediction starting point of 84 (i) B0007 with prediction starting point of 100

Figure 5. RUL prediction of each model on three types of batteries.

Figures 5 (a) to (i) show that, as the prediction start point increases, the CNN-BiGRU model is closer to the true value curve than the other three algorithms, indicating that the CNN-BiGRU algorithm has better battery capacity prediction performance. Tables 9 to 11 list the accuracy tables of the four algorithms at different prediction start points for three batteries. The tables compare the accuracy of the different models and demonstrate the performance of the CNN-BiGRU algorithm in predicting

battery capacity more effectively than the other methods.

The battery prediction results for the CNN-BiGRU, CNN-GRU, GRU, and BiGRU algorithms are compared in Tables 9 to 11 for three batteries (B0005, B0006 and B0007) at various prediction start points. It is observed that the CNN-BiGRU algorithm outperforms the other algorithms in all four evaluation metrics: MAPE, MAE, MSE, and RMSE. Specifically: For battery B0005, the CNN-BiGRU algorithm exhibits MAPE below 0.84%, with MAE ranging between 0.0095 and 0.0511, held an MSE of 0.02% and an RMSE of 0.0178. The performance of the other algorithms, including the CNN-GRU, GRU, and BiGRU, was inferior to the CNN-BiGRU algorithm.

For battery B0006, the performance of the CNN-BiGRU algorithm on all four evaluation metrics is better than those of the CNN-GRU, GRU and BiGRU algorithms. However, it should be noted that the aging process of the B0006 battery accelerated after reaching the failure threshold, which resulted in a rapid decrease in capacity and larger prediction errors.

For battery B0007, the CNN-BiGRU algorithm demonstrated MAPE below 0.87%, MAE below 0.0130 , MSE below 0.0343% and RMSE below 0.0185. Again, the CNN-BiGRU algorithm's performance on all four evaluation metrics was superior to that of the other algorithms.

Therefore, based on the results of the comparison, the CNN-BiGRU algorithm proves more accurate in predicting the capacity of lithium-ion batteries than the other four algorithms. Furthermore, the predicted results of this algorithm are less affected by prediction start point.

Table 9. Capacity prediction result for battery B0005.

Battery	Starting point	Model	MAPE/%	MAE	MSE/%	RMSE
B0005	60	CNN-BiGRU	**0.69%**	**0.0099**	**0.0200**	**0.0141**
		CNN-GRU	1.15%	0.0165	0.0396	0.0199
		GRU	1.33%	0.0188	0.0464	0.0215
		BIGRU	1.53%	0.0216	0.0006	0.0241
B0005	84	CNN-BiGRU	**0.84%**	**0.0118**	**0.0003**	**0.0178**
		CNN-GRU	3.02%	0.0411	0.2316	0.0481
		GRU	0.86%	0.0120	0.0278	0.0167
		BIGRU	1.05%	0.0148	0.0439	0.0210
B0005	100	CNN-BiGRU	**0.69%**	**0.0095**	**0.0199**	**0.0141**
		CNN-GRU	1.05%	0.0145	0.0344	0.0185
		GRU	0.77%	0.0105	0.0175	0.0132
		BIGRU	1.26%	0.0171	0.0337	0.0184

Table 10. Capacity prediction result for battery B0006.

Battery	Starting point	Model	MAPE/%	MAE	MSE/%	RMSE
B0006	60	CNN-BiGRU	**3.23%**	**0.0420**	**0.3560**	**0.0592**
		CNN-GRU	3.74%	0.0491	0.4185	0.0647
		GRU	3.80%	0.0482	0.5271	0.0726
		BIGRU	3.24%	0.0422	0.3578	0.0598
B0006	84	CNN-BiGRU	**4.02%**	**0.0511**	**0.4910**	**0.0701**
		CNN-GRU	4.40%	0.0553	0.6239	0.0790
		GRU	6.12%	0.0774	0.9690	0.0984
		BIGRU	5.52%	0.0698	0.8144	0.0902
B0006	100	CNN-BiGRU	**1.57%**	**0.0204**	**0.0703**	**0.0265**
		CNN-GRU	1.73%	0.0222	0.0772	0.0278
		GRU	6.82%	0.0852	1.0754	0.1037
		BIGRU	8.20%	0.1034	1.3734	0.1172

Table 11. Capacity prediction result for battery B0007.

Battery	Starting point	Model	MAPE/%	MAE	MSE/%	RMSE
B0007	60	CNN-BiGRU	**0.83%**	**0.0128**	**0.0317**	**0.0178**
		CNN-GRU	1.29%	0.0201	0.0689	0.0263
		GRU	0.95%	0.0145	0.0395	0.0199
		BIGRU	1.35%	0.0207	0.0644	0.0254
B0007	84	CNN-BiGRU	**0.87%**	**0.0130**	**0.0343**	**0.0185**
		CNN-GRU	1.34%	0.0197	0.0632	0.0251
		GRU	1.60%	0.0238	0.0727	0.0270
		BIGRU	1.46%	0.0222	0.0707	0.0266
B0007	100	CNN-BiGRU	**0.67%**	**0.0097**	**0.0156**	**0.0125**
		CNN-GRU	2.00%	0.0291	0.1236	0.0352
		GRU	1.30%	0.0190	0.0503	0.0224
		BIGRU	1.75%	0.0256	0.0790	0.0281

According to the analysis in Table 12, the relative error of the remaining life prediction for lithium-ion batteries based on the CNN-BiGRU algorithm using the B0005 battery ranged from 0% to 0.81%, with an absolute error between zero and one. The relative error of RUL prediction based on the CNN-GRU algorithm ranged from 0.81% to 13.71%with an absolute error between one and 17. Similarly, based on the GRU algorithm, the relative error of RUL prediction ranged from 1.61% to 13.71% with an absolute error between two and five. Based on the BiGRU algorithm, the relative error of RUL prediction ranged from 4.84% to 6.45% with an absolute error between six and eight.

Table 12. RUL prediction results for battery B0005.

Battery	Starting point	Model	Real life	Predicted life	Real RUL	Predicted RUL	AE	RE(%)
B0005	60	CNN-BiGRU	124	123	64	63	**1**	**0.81**
		CNN-GRU		125		65	1	0.81
		GRU		128		68	4	3.23
		BiGRU		130		70	6	4.84
B0005	84	CNN-BiGRU	124	124	40	40	**0**	**0.00**
		CNN-GRU		141		57	17	13.71
		GRU		126		42	2	1.61
		BiGRU		117		33	7	5.65
B0005	100	CNN-BiGRU	124	125	24	25	**1**	**0.81**
		CNN-GRU		123		23	1	0.81
		GRU		129		29	5	4.03
		BiGRU		132		32	8	6.45

According to the analysis in Table 13, the relative error of remaining life prediction for the B0006 battery based on the CNN-BiGRU algorithm ranged from 0% to 2.78% with an absolute error between zero and three. The relative error of RUL prediction based on the CNN-GRU algorithm ranged from 0.93% to 12.04% with an absolute error between one and 13. Similarly, based on the GRU algorithm, the relative error of RUL prediction ranged from 7.41% to 18.52% with an absolute error between eight and 20. Based on the BiGRU algorithm, the relative error of RUL prediction ranged from 5.56% to 20.37% with an absolute error between six and 22.

Table 13. RUL prediction results for battery B0006.

Battery	Starting point	Model	Real life	Predicted life	Real RUL	Predicted RUL	AE	RE(%)
B0006	60	CNN-BiGRU	108	108	48	48	**0**	**0.00**
		CNN-GRU		99		39	9	8.33
		GRU		128		68	20	18.52
		BiGRU		102		42	6	5.56
B0006	84	CNN-BiGRU	108	107	24	47	**1**	**0.93**
		CNN-GRU		107		47	1	0.93
		GRU		116		56	8	7.41
		BiGRU		116		56	8	7.41
B0006	100	CNN-BiGRU	108	111	8	51	**3**	**2.78**
		CNN-GRU		121		61	13	12.04
		GRU		116		56	8	7.41
		BiGRU		130		70	22	20.37

According to the analysis in Table 14, the relative error of remaining life prediction for the B0007 battery based on the CNN-BiGRU algorithm ranged from 0% to 2.4%, with an absolute error between zero and three. The relative error of RUL prediction based on the CNN-GRU algorithm

ranged from 1.60% to 7.20% with an absolute error between two and nine. Similarly, based on the GRU algorithm, the relative error of RUL prediction ranged from 3.20% to 7.20% with an absolute error between four and nine. Based on the BiGRU algorithm, the relative error of RUL prediction ranged from 5.60% to 8.00% with an absolute error between eight and nine.

Table 14. RUL prediction results for battery B0007.

Battery	starting point	Model	Real life	predicted life	Real RUL	predicted RUL	AE	RE(%)
B0007	60	CNN-BiGRU	125	122	65	62	**3**	**2.40**
		CNN-GRU		116		56	9	7.20
		GRU		116		56	9	7.20
		BiGRU		115		55	10	8.00
B0007	84	CNN-BiGRU	125	127	41	43	**2**	**1.60**
		CNN-GRU		129		45	4	3.20
		GRU		132		48	7	5.60
		BiGRU		115		31	10	8.00
B0007	100	CNN-BiGRU	125	125	25	25	**0**	**0.00**
		CNN-GRU		123		23	2	1.60
		GRU		129		29	4	3.20
		BiGRU		132		32	7	5.60

In conclusion, when predicting the remaining life of lithium-ion batteries using the CNN-BiGRU algorithm, this approach is more stable and accurate compared to the GRU, BiGRU or CNN-GRU algorithms. This also demonstrates the effectiveness of using the CNN method as a battery health factor for feature extraction, allowing for aging information to be effectively extracted from the battery health factors. The combination of the BiGRU neural network with forward and backward propagation also enables the CNN-BiGRU fusion algorithm to achieve higher accuracy in predicting both the capacity and RUL of the battery.

5. Conclusions

This paper first extracted data from lithium-ion batteries as health factors including the time of isovoltage discharge, average discharge voltage and average temperature and uses them as predictive variables for capacity. Subsequently, the Pearson correlation coefficients between these health factors and capacity were calculated, indicating a high correlation between the three health factors and discharge capacity. This proved that extracting health factors is effective and prepares for predicting the remaining service life of the battery. Furthermore, we proposed a CNN-BiGRU-based indirect prediction model of the remaining service life of lithium-ion batteries and used the TPE adaptive hyperparameter optimization method to optimize the CNN-BiGRU model's hyperparameters. Compared to grid search and manual tuning, the TPE algorithm is more convenient, has a larger hyperparameter search space and provides better results. The experimental results showed that compared to the CNN, GRU and BiGRU algorithms, the CNN-BiGRU algorithm optimized by TPE hyperparameters achieved higher accuracy in predicting the remaining service life of lithium-ion batteries without requiring manual parameter adjustment.

This study achieved certain results in predicting the health status and remaining useful life of lithium-ion batteries, but there are still some shortcomings and room for improvement. Because the model fusion used in this study is the fusion of two data-driven models, future research can use the method of fusing physical and data-driven models to study the health status and remaining service life of lithium-ion batteries and increasing the model's interpretability. Next, this study did not consider the impact of environmental temperature on the prediction of battery health status and remaining service life. Future experiments can be conducted to analyze temperature's effect on lithium-ion batteries.

Use of AI tools declaration

The authors declare they have not used Artificial Intelligence (AI) tools in the creation of this article.

Acknowledgments

This work is jointly supported by the National Natural Science Foundation of China under Grant 61976055, the Third Batch of Innovative Star Talent Plan in Fujian Province under Grant 003002, the Special Fund for Education and Scientific Research of Fujian Provincial Department of Finance under Grant GY-Z21001 and the Scientific Research Foundation of Fujian University of Technology under Grant GY-Z22071.

Conflict of interest

No potential conflict of interest was reported by the authors.

References

1. Chen M, Rincon-Mora GA (2006) Accurate electrical battery model capable of predicting runtime and iv performance. *IEEE Trans Energy Convers* 21: 504–511. https://doi.org/ 10.1109/TEC.2006.874229
2. Chen L, Xu C, Bao X, et al. (2023) State-of-health estimation of Lithium-ion battery based on back-propagation neural network with adaptive hidden layer. *Neural Comput Appl* 35: 14169–14182. https://doi.org/10.1007/s00521-023-08471-7
3. Goodenough JB, Park KS (2013) The Li-ion rechargeable battery: a perspective. *J Am Chem Soc* 135: 1167–1176. https://doi.org/10.1021/ja3091438
4. Liu Z, He B, Zhang Z, et al. (2022) Lithium/graphene composite anode with 3d structural lif protection layer for high-performance lithium metal batteries. *ACS Appl Mater Interfaces* 14: 2871–2880. https://doi.org/10.1021/acsami.1c21263
5. Fei Z, Zhang Z, Yang F, et al. (2022) Early-stage lifetime prediction for lithium-ion batteries: A deep learning framework jointly considering machine-learned and handcrafted data features. *J Energy Storage* 52: 104936. https://doi.org/10.1016/j.est.2022.104936

6. Basia A, Simeu-Abazi Z, Gascard E, et al. (2021) Review on state of health estimation methodologies for lithium-ion batteries in the context of circular economy. *CIRP J Manuf Sci Technol* 32: 517–528. https://doi.org/10.1016/j.cirpj.2021.02.004
7. Ma J, Zou XY, Sun L, et al. (2023) A prediction-based cycle life test optimization method for cross-formula batteries using instance transfer and variable-length-input deep learning model. *Neural Comput Appl* 35: 2947–2971. https://doi.org/10.1007/s00521-022-07322-1
8. Ge MF, Liu Y, Jiang X, et al. (2021) A review on state of health estimations and remaining useful life prognostics of lithium-ion batteries. *Meas* 174: 109057. https://doi.org/10.1016/j.measurement.2021.109057
9. Hu C, Youn BD, Wang P, et al. (2012) Ensemble of data-driven prognostic algorithms for robust prediction of remaining useful life. *Reliab Eng System Safety* 103: 120–135. https://doi.org/10.1016/j.ress.2012.03.008
10. Jarid S, Das M (2021) An electro-thermal model based fast optimal charging strategy for Li-ion batteries. *AIMS Energy* 9: 915–933. https://doi: 10.3934/energy.2021043
11. Ma G , Zhang Y, Cheng C, et al. (2019) Remaining useful life prediction of lithium-ion batteries based on false nearest neighbors and a hybrid neural network. *Appl Energy* 253: 113626. https://doi.org/10.1016/j.apenergy.2019.113626
12. Fei Z, Zhang Z, Yang F, et al. (2023) A deep attention-assisted and memory-augmented temporal convolutional network based model for rapid lithium-ion battery remaining useful life predictions with limited data. *J Energy Storage* 62: 106903. https://doi.org/10.1016/j.est.2023.106903
13. Lyu C, Lai Q, Ge T, et al. (2017) A lead-acid battery's remaining useful life prediction by using electrochemical model in the particle filtering framework. *Energy* 120: 975–984. https://doi.org/10.1016/j.energy.2016.12.004
14. Wang S, Jin S, Bai D, et al. (2021) A critical review of improved deep learning methods for the remaining useful life prediction of lithium-ion batteries. *Energy Rep* 7: 5562–5574. https://doi.org/10.1016/j.egyr.2021.08.182
15. Khare N, Singh P, Vassiliou JK (2012) A novel magnetic field probing technique for determining state of health of sealed lead-acid batteries. *J Power Sources* 218: 462–473. https://doi.org/10.1016/j.jpowsour.2012.06.085
16. Mevawalla A, Shabeer Y, Tran MK, et al. (2022) Thermal modelling utilizing multiple experimentally measurable parameters. *Batteries* 8: 147. https://doi.org/10.3390/batteries8100147
17. Wang Y, Dan D, Zhang Y, et al. (2022) A novel heat dissipation structure based on flat heat pipe for battery thermal management system. *Int J Energy Res* 46: 15961–15980. https://doi.org/10.1002/er.8294
18. Xie Y, Li W, Hu X, et al. (2022) Coestimation of soc and three-dimensional sot for lithium-ion batteries based on distributed spatial–temporal online correction. *IEEE Trans Ind Electron* 70: 5937–5948. https://10.1109/TIE.2022.3199905
19. Xing Y, Williard N, Tsui KL, et al. (2011) A comparative review of prognostics-based reliability methods for lithium batteries. *2011 Prognostics and System Health Managment Confernece* https://10.1109/PHM.2011.5939585

20. Wang D, Yang F, Tsui KL, et al. (2016) Remaining useful life prediction of lithium-ion batteries based on spherical cubature particle filter. *IEEE Trans Instrum Meas* 65: 1282–1291. https://10.1109/TIM.2016.2534258

21. Tran MK, DaCosta A, Mevawalla A, et al. (2021) Comparative study of equivalent circuit models performance in four common lithium-ion batteries: Lfp, nmc, lmo, nca. *Batteries* 7: 51. https://doi.org/10.3390/batteries7030051

22. Fei Z, Zhang Z, Yang F, et al. (2023) A deep attention-assisted and memory-augmented temporal convolutional network based model for rapid lithium-ion battery remaining useful life predictions with limited data. *J Energy Storage* 62: 106903. https://doi.org/10.1016/j.est.2023.106903

23. Wang S, Ren P, Takyi-Aninakwa P, et al. (2022) A critical review of improved deep convolutional neural network for multi-timescale state prediction of lithium-ion batteries. *Energies* 15: 5053. https://doi.org/10.3390/en15145053

24. Chun H, Yoon K, Kim J, et al. (2022) Improving aging identifiability of lithium-ion batteries using deep reinforcement learning. *IEEE Trans Transp Electrif* 9: 995–1007. https://10.1109/TTE.2022.3186151

25. Kim J, Chun H, Kim H, et al. (2023) Strategically switching metaheuristics for effective parameter estimation of electrochemical lithium-ion battery models. *J Energy Storage* 64: 107094. https://doi.org/10.1016/j.est.2023.107094

26. Cai L, Meng J, Stroe DI, et al. (2020) Multiobjective optimization of data-driven model for lithium-ion battery soh estimation with short-term feature. *IEEE Trans Power Electron* 35: 11855–11864. https://10.1109/TPEL.2020.2987383

27. Qin T, Zeng S, Guo J (2015) Robust prognostics for state of health estimation of lithium-ion batteries based on an improved pso–svr model. *Microelectron Reliab* 55: 1280–1284. https://doi.org/10.1016/j.microrel.2015.06.133

28. Cai Y, Yang L, Deng Z, et al. (2017) Prediction of lithium-ion battery remaining useful life based on hybrid data-driven method with optimized parameter. *2017 2nd International Conference on Power and Renewable Energy*. https://10.1109/ICPRE.2017.8390489

29. Fei Z, Zhang Z, Tsui KL (2023) Deep learning powered online battery health estimation considering multi-timescale ageing dynamics and partial charging information. *IEEE Trans Transp Electrif*. https://doi.org/10.1109/TTE.2023.3264438

30. Ma G, Zhang Y, Cheng C, et al. (2019) Remaining useful life prediction of lithium-ion batteries based on false nearest neighbors and a hybrid neural network. *Appl Energy* 253: 113626. https://doi.org/10.1016/j.apenergy.2019.113626

31. Zhang Y, Xiong R, He H, et al. (2018) Long short-term memory recurrent neural network for remaining useful life prediction of lithium-ion batteries. *IEEE Trans Veh Technol* 67: 5695–5705. https://doi.org/10.1109/TVT.2018.2805189

32. Yalçın S, Panchal S, Herdem MS (2022) A cnn-abc model for estimation and optimization of heat generation rate and voltage distributions of lithium-ion batteries for electric vehicles. *Int J Heat Mass Transfer* 199: 123486. https://doi.org/10.1016/j.ijheatmasstransfer.2022.123486

33. Wang F, Zhao Z, Ren J, et al. (2022) A transferable lithium-ion battery remaining useful life prediction method from cycle-consistency of degradation trend. *J Power Sources* 521: 230975. https://doi.org/10.1016/j.jpowsour.2022.230975

34. Chen D, Zheng X, Chen C, et al. (2022) Remaining useful life prediction of the lithium-ion battery based on cnn-lstm fusion model and grey relational analysis. *Electron Res Arch* 31: 633–655. https://doi.org/10.1177/01423312221114506

35. Xia M, Zheng X, Imran M, et al. (2020) Data-driven prognosis method using hybrid deep recurrent neural network. *Appl Soft Computing* 93: 106351. https://doi.org/10.1016/j.asoc.2020.106351

36. Yao F, He W, Wu Y, et al. (2022) Remaining useful life prediction of lithium-ion batteries using a hybrid model. *Energy* 248: 123622. https://doi.org/10.1016/j.energy.2022.123622

37. Zhou W, Lu Q, Zheng Y (2022) Review on the selection of health indicator for lithium ion batteries. *Mach* 10: 512. https://doi.org/10.3390/machines10070512

38. Xu H, Peng Y, Su L (2018) Health state estimation method of lithium ion battery based on nasa experimental data set. *IOP Conference Series: Materials Science and Engineering* https://doi.org/10.1088/1757-899X/452/3/032067

39. Wu W, Lu S (2023) Remaining useful life prediction of lithium-ion batteries based on data preprocessing and improved elm. *IEEE Trans Instrum Meas* https://doi.org/10.1109/TIM.2023.3267362

40. Chen L, Zhang Y, Zheng Y, et al. (2020) Remaining useful life prediction of lithium-ion battery with optimal input sequence selection and error compensation. *Neurocomput* 414: 245–254. https://doi.org/10.1016/j.neucom.2020.07.081

41. Bischl B, Binder M, Lang M, et al. (2023) Hyperparameter optimization: Foundations, algorithms, best practices, and open challenges. *Wiley Interdiscip Rev: Data Min Knowl Discovery* 13: e1484. https://doi.org/10.1002/widm.1484

42. Ioannou G, Tagaris T, Stafylopatis A (2023) Adalip: An adaptive learning rate method per layer for stochastic optimization. *Neural Process Lett* 2023: 1-28. https://doi.org/10.1007/s11063-022-11140-w